

OBSERVED NEAR-SURFACE WIND FLOW CHARACTERISTICS OF GULF COAST HURRICANES: 2004-2008

Ian M. Giammanco^{1*}, Juan-Antonio Balderrama², John L. Schroeder¹, Forrest J. Masters², and
Peter J. Vickery³

¹ Texas Tech University, Lubbock, Texas

² University of Florida, Gainesville, Florida

³ Applied Research Associates, Raleigh, North Carolina

1. INTRODUCTION

Since 1998 university programs have deployed ruggedized observing systems into the path of landfalling hurricanes to collect research grade measurements of the near-surface wind flow. Data records from these platforms represent a large percentage of the complete wind records from the most notable landfalling tropical cyclones of the past decade. The current study leverages observations from landfalling hurricanes along the Gulf Coast of the United States from 2004-2008 collected by the Florida Coastal Monitoring Program (FCMP), Texas Tech University's (TTU) Wind Engineering Mobile Instrument Tower Experiment (WEMITE), and the TTU's StickNet adaptive observing network (Schroeder and Smith 2003; Weiss and Schroeder 2008; Masters et al. 2010; Balderrama et al. 2011). The combined data archive contained over 90 complete high-resolution (sampling rate ≥ 1 Hz) wind records and represents the largest archive assembled to examine near-surface wind flow characteristics. The study focused on examining secondary influences to the near-surface wind flow beyond those associated with changes in upstream terrain. Emphasis was placed on examining these characteristics in relatively smooth surface roughness conditions.

Historical literature has shown the turbulent fluctuations of the hurricane boundary layer (HBL) wind flow are strongly influenced by mechanical mixing as a result of the upstream terrain conditions (Vickery and Skerlj 2005; Paulsen and Schroeder 2005; Schroeder et al. 2009). Perturbations from the mean flow are dominated by the mechanical production of turbulence while buoyancy effects are limited due to neutral stratification.

Recent work by Schroeder et al (2009) has provided observational evidence of secondary influences on the wind flow characteristics as a result of storm-relative position. Large changes to the wind flow characteristics within a single data record are typically a result of changing upstream surface roughness conditions as the wind direction evolves over the course of a tropical cyclone landfall.

2. DATA, QUALITY CONTROL, AND METHODOLOGY

Data were separated by measurement height (10 m height for WEMITE and FCMP platforms and 2.25 m for StickNet probes). Observations were fully segmented using a 10-minute window to calculate the wind flow characteristics (e.g. turbulence intensity, gust factor, longitudinal integral length scale). Although methodology exists to standardize mean wind speeds to a common measurement height, the turbulence parameters cannot be adjusted. For each 10 minute segment, a gust factor, turbulence intensity, and longitudinal integral length scale were calculated. Gust factors were defined as the ratio of the peak 3-second gust within the 10-minute block of data to the mean wind speed of the segment in accordance with typical wind engineering applications.

Each high resolution data record was subjectively reviewed following deployment to ensure its quality. Time histories were also subjected to a range test and observations which fell outside ± 3 standard deviations of a one-minute mean value were flagged. Each ten minute segment of data was also subjected to a non-parametric run test utilizing a 95% confidence interval to ensure there was no significant trend within the window. Following the quality control procedures, 3590 ten-minute data segments at 10 m height and 11,743 data segments for 2.25 m observations were available for analysis. Table 1 provides a list of the landfalling tropical cyclones included and the available number of quality controlled 10-minute data segments.

In order to document the influence of upstream terrain as well as to extract changes as a result of

*Corresponding Author Address:

Ian M. Giammanco, Ph.D.

Now: Insurance Institute for Business and Home Safety
Richburg, South Carolina, 29729

igiammanco@ibhs.org

Phone: (803) 789-4207

other mechanisms beyond frictional effects, 10-minute segments of data were stratified into three surface roughness categories based on those used by Schroeder et al. (2009) (Table 2). Surface roughness lengths (Z_0) for each 10-minute data segment were computed using the turbulence intensity method which assumes neutral stratification and a constant ratio of frictional velocity to the wind speed standard deviation ($\sigma_v/u_* = 2.5$; Beljaars 1987). Observations which fell into the rough terrain category were removed from the analysis as the current study's focus was on wind flow characteristics in relatively smooth roughness regimes. Within each roughness classification, additional stratifications were applied to investigate the influence of mean wind speed, radial distance from the cyclone center, and precipitation structure on the turbulence quantities.

The use of the turbulence intensity (TI) method to determine the roughness length allowed it to vary temporally with changes in wind speed and no change in upstream fetch. The use of a 10-minute data segment helped mitigate the influence of a time-varying quantitative roughness approach. A qualitative roughness assessment through aerial photography has been shown to produce large errors and often can result in a bias toward rougher terrain (Weiringa 1992; Powell et al. 1996; Schroeder et al. 2009). Using only WEMITE data at 10 m observation height Schroeder et al. (2009) found that no 5-minute data segments fell into the smooth category when using the qualitative roughness assessment.

3. MEAN WIND SPEED INFLUENCES

The stratification of observations into their respective roughness regimes allowed for secondary dependencies to be identified. Within neutrally stratified boundary layers, the influence of mean wind speed upon the turbulent wind flow characteristics is expected to be minimal given that all other properties remain constant (e.g. upstream roughness conditions, absence of convective motions). Gust factors, longitudinal turbulence intensity, and longitudinal integral length scales were examined as a function of mean wind speed (10-minute mean). Observations within each roughness regime were segregated using 5 m s^{-1} bin sizes into the following groups: 0-4.99, 5-9.99, 10-14.99, 15-19.99, 20-24.99, 25-29.99, and 30-34.99 m s^{-1} .

A general trend of decreasing gust-factors with increasing mean wind speed was observed for both 10 m and 2.25 m observations (Figure 1). This relationship was evident for all three roughness regimes but was most pronounced within the open and roughly open categories with a decrease of 7% and 5% respectively for bin-averaged gust factors from 10-30 m s^{-1} for 10 m observations (Figure 2). The mean gust factor values for 2.25 m observations exhibited a more significant decrease of 11% within the smooth exposure classification between 10 and 30 m s^{-1} . However, the sample size of the 30-34.99 m s^{-1} group was only 3 observations. The range of

gust factors was also somewhat dependent upon mean wind with an observed decrease. Between the three roughness classifications, the mean gust factors tended to converge as 10-minute mean wind speeds increased above 15 m s^{-1} . It was noted that 10 m mean wind speeds did not exceed 30 m s^{-1} within the roughly open classification and did not exceed 20 m s^{-1} for 2.25 m observations. The mean and standard deviation for each group is provided in Figure 2. The mean longitudinal turbulence intensities remained relatively constant with wind speed. A slight decrease of 1% and 2% was noted for 10 m and 2.25 m observations respectively (Figure 2). The result was expected given the typical properties of neutrally stratified boundary layers. One exception was found within the smooth exposure classification for 2.25 m observations; a decrease of 5% between mean wind speeds of 10 and 30 m s^{-1} was observed. The result however was likely influenced by the very small sample size for the highest wind speed group.

Longitudinal integral length scales exhibited an increase with mean wind speed and increased for all roughness classifications (Figure 2). For 10 m observations within the smooth classification, the mean value leveled off near 200 m. The 2.25 m observations showed a similar trend but with slightly shorter length scales due to the lower measuring height. As shown in Figure 3, longitudinal integral length scales exhibited significant perturbations and standard deviations were quite large. The largest eddy sizes were identified within the smooth category and were approximately 850 and 700 m for 10 m and 2.25 m observations, respectively. The influence of frictional effects was evident as the shortest eddy sizes were confined to the roughly open terrain exposure category.

4. STORM- RELATIVE POSITION

Theoretical and observational literature has shown that the structure of the hurricane boundary layer can change with azimuth and radial distance from the storm center (Kepert 2001; Kepert and Wang 2001; Kepert 2006a,b; Schwendike and Kepert 2008; Zhang et al. 2011; Giammanco et al. 2012). The depth of the boundary layer and the associated wind speed maximum was found to decrease toward the cyclone center (Kepert 2006a,b; Zhang et al. 2011; Giammanco et al. 2012). It was also suggested by Powell et al. (2003) that the wind maximum aloft was a reasonable upper-bound for expected near-surface gust values. The wind speed maximum aloft within composite profiles decreased in relative magnitude with radial distance, suggesting that surface gust factors may respond in a similar fashion (Zhang et al. 2011; Giammanco et al. 2012). Observational evidence exists to support the hypothesis that the near-surface wind flow is also dependent on storm-relative position (Schroeder et al. 2009). The current study employs a significantly larger dataset than historical research to investigate this question.

The large size of the dataset allowed for a comprehensive examination of the changes in the wind flow characteristics with changes in storm-relative position. A radial distance was assigned to each 10-minute data segment using the method described by Willoughby and Chelmow (1982) to compute storm-relative position (e.g. radius and azimuth). Observations for each measuring height and roughness classification were stratified by radial distance from the cyclone center by the following groups: < 40 km, 40-80 km, 80-150 km, 150-250 km, 250-400 km, and > 400 km.

Gust factor values tended to increase moving radially outward from the cyclone center, as shown in Figure 4. It was particularly evident for observations at 10m; whereas at 2.25 m, the trend was present but not statistically significant. The lack of an identifiable relationship for 2.25 m observations suggested that the influence of dynamical processes likely increases with height in the HBL boundary layer. The result was anticipated as the influence of frictional processes is a maximum close to the surface and decreases with height. The mean gust factors increased the most significantly at radii greater than 150 km. It is noted that at radii greater than 400 km, the mean wind flow was likely more representative of the synoptic-scale wind conditions and not directly attributed to the cyclone circulation.

The open and roughly-open classifications exhibited the most visible trend toward larger gust factors. This effect was also evident within the mean values when observations were binned by radius (Figure 5). The open and roughly open classifications exhibited the sharpest increase in gust factor values as radial distance increased. The trend was not pronounced within the 2.25 m mean values; only a slight increase of 3% for the open and roughly open flow regimes was found.

The longitudinal integral length scale values also responded to changes in radial distance. For 10 m observations, a trend toward smaller eddy lengths with larger radii was observed (Figure 6). The mean values for the radial groupings also contained a similar relationship with the open classification being the most evident (Figure 7). Mean length scales typically decreased from 150-200 m at the smallest radii to near 75-80 m well removed from the cyclone center. The trend was not present within the 2.25 m observations from the open and roughly open classifications as mean integral length scale values remained nearly constant. Only a small decrease of 30 m in length scale was observed within the smooth classification. It is noted that integral length scale values were found to be more variable than gust-factors or turbulence intensities.

Mean turbulence intensity values for 10 m observations increased with radial distance for the open and roughly open classifications. The increase was 5% and 6% respectively. The smooth exposure class exhibited a non-significant 1% change across the five radial groups. For 2.25 m observations there was only a 1% change noted within the smooth exposure classification while the remaining two

classifications remained constant with increasing radial distance.

5. PRECIPITATION STRUCTURE

The influence of convective features on the near-surface gust characteristics has been mentioned within historical literature. Fujita (1985) speculated that convective downburst features could contribute to "extreme" near-surface wind gusts (gust factors > 2.00) and observed damage gradients. Observational studies have found these to be extremely rare (Bradbury et al. 1994; Sparks and Huang 2001; Schroeder and Smith 2003; Paulsen and Schroeder 2005; Vickery and Skerlj 2005; Schroeder et al. 2009). Within a tropical cyclone, deep convection is typically confined to the eyewall region at small radii and within convective rainband features at large radii (Jorgensen 1984b). The effect of buoyancy driven gusts within outer rainbands, from an engineering perspective, is considered to be minimal given the relatively weak mean wind environment in which they occur. Although large gust factors may occur, gust wind speeds in this region are not anticipated to exceed minimum structural design standards. The primary concern lies within the eyewall region at relatively small radii.

Composite radar reflectivity data from coastal WSR-88D radars were assimilated with the near surface observations to investigate the influence of precipitation structure and eyewall passages on the wind flow characteristics. The precipitation structure was examined and characterized for each ten-minute wind segment using radar volumes which fell within the window using a qualitative assessment (e.g. convective or stratiform). Additionally, observations were also given a subjective outer-vortex or eyewall classification. Composite radar reflectivity data were interrogated to locate horizontal gradients as well as to identify the melting level (i.e. bright band) within vertical cross-sections over the observation platform. Both features are indicative of convective precipitation (Houze 1997). If no determination could be made, the observation was not assigned to a group. The methodology follows that of Schroeder et al. (2009).

For smooth terrain exposure and 10 m measuring height, little change in mean gust factors was observed; however the range of gust factors decreased for eyewall observations. It is noted that for observations classified as "eyewall", gust factors did not exceed 1.79 (Table 3). Within the open and roughly open classifications, the mean gust factor was a maximum for outer-vortex convective regions with a minimum for eyewall observations. Observations at 2.25 m contained a similar trend within the roughness classes (Table 4). The result mirrored the radial dependence previously described but also indicated that convective features within outer bands contribute to larger near-surface gust factors. The slight difference between the two measuring heights may simply be due to the larger sample size provided by the 2.25 m (StickNet) dataset and the increase in frictional effects at the

lower measuring height. These relationships were reflected in the mean longitudinal turbulence intensities but differences were only 1-2% between categories. The mean integral length scales also exhibited a dependence on precipitation structure. The eyewall region contained the longest mean eddy sizes and the shortest were found within the outer-vortex stratiform regime. Integral length scales were found to be somewhat variable with large ranges and standard deviations. It is speculated that integral length scales respond much more readily to the evolving precipitation structure. Gust factor and turbulence intensity values do not exhibit significant changes. The temporal resolution of WSR-88D volumetric scanning strategies did not allow for these small-scale changes to be examined.

Composite reflectivity time histories for the radar volume over each platform's location were directly compared to near-surface observations to examine the influence of enhanced reflectivity and the near surface wind field. Composite reflectivity from the radar volume closest to the peak 3-second gust was assigned to each 10-minute data segment. Observations at 10 m revealed a slight increase in gust factor values with increasing composite reflectivity within the open and roughly open flow regimes; 2.25 m observations contained no trend (Figure 8). The identified linear trend was not found to be statistically significant. When binned by reflectivity according to Schroeder et al. (2009), the mean gust factors showed little dependence at both the 10 m and 2.25 m observation heights for all three exposure classifications. The mean turbulence intensity values also showed little relationship. Integral length scales were again quite variable. The result differed from that found by Schroeder et al. (2009); who identified a slight increase in longitudinal integral length scales with increasing reflectivity. The difference may be a result of the shorter averaging time applied to surface observations (5-minutes) by Schroeder et al. (2009). The 5-minute time averaging period corresponds well with the time required for the WSR-88D to complete its volumetric sampling strategy. The 10-minute window employed by the current study at times included two complete radar volumes or a second volume had begun prior to the end of the data segment. In addition, the precipitation structure often changed significantly between radar volumes and individual features other than cellular outer rainband convection were difficult to track through multiple radar volume scans.

6. SUMMARY AND DISCUSSION

The deployment of ruggedized observing systems by Texas Tech University and the Florida Coastal Monitoring Program yielded a significant number of data records in which gust factors (3-second/10-minute), longitudinal turbulence intensity, and longitudinal integral length scales could be calculated and interrogated. These quantities were used to describe the horizontal wind flow characteristics. Observations were placed into a storm-relative framework in order to examine the

influence of radial position. These data were synthesized with WSR-88D radar reflectivity records to study the influence of precipitation structure aloft on the local wind field. Stratifying observations into exposure categories and grouping by mean wind speed and radial distance allowed for secondary relationships to become evident.

Gust factors and turbulence intensities tended to decrease as mean winds increased and radial distance increased. The two stratifications are linked given that the strongest winds are typically found at small radii within the eyewall region. It is noted that observations made at 10 m height (WEMITE, FCMP) responded to secondary influences, beyond frictional effects, than those collected at 2.25 m (StickNet). Within the eyewall region mean longitudinal length scales generally increased. Although speculation within historical literature has suggested the hurricane eyewall is a region of anomalous gusts, the current study does not support this hypothesis. One could argue that the eyewall region is slightly less turbulent or no different in turbulent character than the other regions of a hurricane. Eyewall observations tended to have the lowest average gust factors and largest integral length scales while outer-vortex convective observations did produce a large length scale and slightly larger gust factors than those found in stratiform conditions. It is noted that gust factor values did not exceed 2.00 for any eyewall observation from the three roughness classifications and the two different measuring heights. The results argued that within the three roughness regimes large gust factors were confined to large radii. Such instances are of little concern within the engineering community as they occur within a relatively low wind speed environment.

The radial dependence noted in this study and by Schroeder et al. (2009) was strikingly similar to the change in the relative magnitude of the wind speed maximum aloft found in composite vertical wind profiles (Giammanco et al. 2012). It is hypothesized that given a decreasing scaled wind maximum aloft at small radial distances the vertical momentum available for transport to the surface as a gust feature is reduced. This may help explain the relative lack of extreme (gust factor > 2.0) gusts within the eyewall region. It is noted that Kepert (2006a,b) suggested that the character of the wind maximum aloft is likely influenced by storm size through the shape of the radial profile of the gradient wind. It is suspected that the near-surface wind flow characteristics may also follow a similar trend.

No relationship was noted between the turbulent quantities and composite reflectivity values and identifying any direct relationship between WSR-88D composite reflectivity and turbulence quantities was difficult. Although Schroeder et al. (2009) found a slight increase in gust factor and integral length scales with increasing composite reflectivity, the current study could not identify any statistically significant trends. It is possible the difference may be a result of the larger sample size or the longer data window (10-minute) used by the current study. The

lack of a coherent trend within the large dataset discouraged the use of WSR-88D radar composite reflectivity to imply any information about the underlying near-surface wind field characteristics. The configurable scanning strategies offered by mobile research radar platforms would be a more appropriate tool to investigate the influence of the rapidly changing precipitation structure on the near-surface wind field. The use of disdrometer and particle imaging systems on mobile research platforms can also aid in investigating the influence of changing precipitation structure.

The near-surface observations presented here represent the largest archive of tropical cyclone wind measurements ever assembled to date. However, the data are primarily representative of over-land exposures. Unfortunately only a small fraction of the archive was collected in true marine exposure conditions and in 10-minute mean wind speeds in excess of 35 m s^{-1} . There remains a significant need to collect critical near-surface measurements in both over-land and marine exposure conditions in higher mean wind speeds to determine if similar storm-relative influences exist. Additional work is also needed to understand the relationship between the near-surface wind field and associated vertical wind profiles.

ACKNOWLEDGEMENTS

Financial support for the analysis efforts was provided by Chevron and Applied Research Associates. Texas Tech University data collection efforts were funded through NIST Cooperative Agreement Award (70NANB8H0059) and NSF (ATM-0134188). Florida Coastal Monitoring Program activities were supported in part by NSF under Grants nos. CMMI-0625124, CMMI-1055744 and CMMI-0928563.

REFERENCES

- Balderrama, J.A., Masters, F.J., Gurley, K.R., Prevatt, D.O., Aponte-Bermudez, L., Reinhold, T.A., Pinelli, J-P., Subramanian, C.S., Schiff, S.D., and Chowdhury, A.G., 2011: The Florida Coastal Monitoring Program: A review. *J. Wind Eng. Indus. Aerodyn.*, **99**, 979-999.
- Beljaars, A. C. M., 1987: The measurement of gustiness at routine wind stations – a review. Scientific Report WR87-11, KNMI, de Bilt, Netherlands.
- Fujita, T.T., 1992: Damage survey of Hurricane Andrew in south Florida. *Storm Data*, **34**, 176 pp.
- Giammanco, I.M., Schroeder, J.L., and Powell, M.D., 2012: Observed characteristics of tropical cyclone vertical wind profiles. *J. Wind and Struc.*, **15**, 1-22.
- Houze, R. A., Jr., 1997: Stratiform precipitation in regions of convection: A meteorological paradox?. *Bull. Amer. Meteor. Soc.*, **78**, 2179-2196.
- Jorgensen, D.P., 1984: Mesoscale and convective scale characteristics of mature hurricanes, Part II: Inner core structure of Hurricane Allen (1980), *J. Atmos. Sci.*, **41**, 1287-1311.
- Kepert, J.D., 2001: The dynamics of boundary layer jets within the tropical cyclone core. Part I: Linear theory. *J. Atmos. Sci.* **58**, 2469-2483.
- Kepert, J.D. and Wang, Y., 2001: The dynamics of boundary layer jets within the tropical cyclone core. Part II: Non-linear enhancement. *J. Atmos. Sci.*, **58**, 2469-2483.
- Kepert, J.D., 2006: Observed boundary layer wind structure and balance in the hurricane core Part II: Hurricane Mitch. *J. Atmos. Sci.*, **63**, 2169-2193.
- Masters, F., Tieleman, F., and Balderrama, J.A. 2010: Surface wind measurements in three Gulf Coast hurricanes of 2005, *J. Wind Eng. Ind. Aerodyn.*, **98**, 533-547.
- Powell, M.D., Houston, S.H., and Reinhold, T.A., Hurricane Andrew's landfall in South Florida, Part I: Standardizing measurements for documenting surface wind fields. *Wea. Forecast.*, **11**, 304-327.
- Powell, M.D., Vickery, P.J. and Reinhold, T.A. 2003: Reduced drag coefficients for high wind speeds in tropical cyclones. *Nature*, **422**, 279-283.
- Schroeder, J.L. and Smith, D.A., 2003: Hurricane Bonnie wind flow characteristics. *J. Wind Eng. Ind. Aerodyn.*, **91**, 767-789.
- Schroeder, J.L., Paulsen-Edwards, B., Giammanco, I.M., 2009: Observed tropical cyclone wind flow characteristics, *J. Wind Struc.*, **17**, 349-382.
- Schwendike, J. and Kepert, J.D. 2008: The boundary layer winds in Hurricanes Danielle (1998) and Isabel (2003). *Mon. Wea. Rev.*, **136**, 3168-3192.
- Sparks, P.R. and Huang, Z., 2001: Gust factors and surface-to-gradient wind-speed in tropical cyclones, *J. Wind Eng. Ind. Aerodyn.*, **89**, 1047-1058.
- Weiringa, J., 1992: Updating the Davenport roughness classification, *J. Wind. Eng. Ind. Aerodyn.*, **41**, 357-368.
- Zhang, J., Rogers, R.F., Nolan, D.S., and Marks, F.D., 2011: On the characteristic height scales of the hurricane boundary layer. *Mon. Wea. Rev.*, **139**, 2523-2535.

Table 1. List of available ten-minute data segments for each landfalling hurricane and program.

Hurricane	Program	Number of Platforms	10-min data records available
Charley (2004)	FCMP	2	76
Ivan (2004)	FCMP	3	282
Ivan (2004)	TTU-WEMITE	4	620
Dennis (2005)	FCMP	3	414
Katrina (2005)	FCMP	3	335
Katrina (2005)	TTU-WEMITE	3	465
Rita (2005)	FCMP	3	320
Rita (2005)	TTU-WEMITE	4	696
Dolly (2008)	TTU-StickNet	22	4491
Gustav (2008)	FCMP	4	384
Gustav (2008)	TTU -StickNet	19	3221
Ike (2008)	FCMP	5	618
Ike (2008)	TTU-StickNet	23	3411

Table 2. Roughness categories according to Schroeder et al. (2009) and total 10-minute data segments for each observation height.

Roughness Regime	Roughness Length (Z_o)	Total 10 m Data Segments	Total 2.25 m Data Segments
Smooth	$0.005 \leq Z_o \leq 0.0199$	1254	7131
Open	$0.02 \leq Z_o \leq 0.0499$	745	2687
Roughly- Open	$0.05 \leq Z_o \leq 0.1899$	461	778

Table 3. 10m observations (WEMITE, FCMP) gust factor (3-sec/10-min) statistics (A), longitudinal turbulence intensity (TI) statistics (B), and longitudinal integral length scale statistics (C) for smooth, open, and roughly open exposures stratified by precipitation structure (convective/ stratiform) and eyewall or outer-vortex. The mean wind speed (m s^{-1}) for each group is also included.

A.			
Statistic	Eyewall	Outer Vortex- Stratiform	Outer Vortex- Convective
Gust Factor- Smooth			
Mean	1.43	1.43	1.44
Maximum	1.64	1.82	1.85
Minimum	1.27	1.20	1.20
Standard Deviation	0.11	0.09	0.11
Mean Wind Speed	26.1	17.5	17.9
Sample Size	20	516	220
Gust Factor – Open			
Mean	1.51	1.52	1.56
Maximum	1.79	1.92	1.94
Minimum	1.34	1.31	1.35
Standard Deviation	0.09	0.11	0.13
Mean Wind Speed	23.4	15.5	17.6
Sample Size	34	315	220
Gust Factor – Roughly Open			
Mean	1.54	1.57	1.61
Maximum	1.63	2.14	2.07
Minimum	1.45	1.34	1.39
Standard Deviation	0.06	0.11	0.14
Mean Wind Speed	21.5	14.1	15.2
Sample Size	16	192	98
B.			
Statistic	Eyewall	Outer Vortex- Stratiform	Outer Vortex- Convective
TI- Smooth			
Mean	0.17	0.16	0.16
Maximum	0.20	0.21	0.21
Minimum	0.13	0.09	0.09
Standard Deviation	0.02	0.02	0.02
Mean Wind Speed	26.1	17.5	17.9
Sample Size	20	516	220
TI – Open			
Mean	0.18	0.19	0.20
Maximum	0.25	0.26	0.26
Minimum	0.16	0.16	0.16
Standard Deviation	0.02	0.03	0.03
Mean Wind Speed	23.4	15.5	17.6
Sample Size	34	315	220
TI – Roughly Open			
Mean	0.20	0.21	0.22
Maximum	0.21	0.30	0.31
Minimum	0.19	0.19	0.19
Standard Deviation	0.007	0.03	0.03
Mean Wind Speed	21.5	14.1	15.2
Sample Size	16	192	98

C.

Statistic	Eyewall	Outer Vortex- Stratiform	Outer Vortex- Convective
Longitudinal Integral Scale- Smooth			
Mean	172	129	138
Maximum	340	653	455
Minimum	82	33	34
Standard Deviation	76	66	83
Mean Wind Speed	26.1	17.5	17.9
Sample Size	20	516	220
Longitudinal Integral Scale– Open			
Mean	236	106	124
Maximum	391	395	336
Minimum	113	40	47
Standard Deviation	120	75	53
Mean Wind Speed	23.4	15.5	17.6
Sample Size	34	315	220
Longitudinal Integral Scale – Roughly Open			
Mean	256	124	141
Maximum	388	252	298
Minimum	126	64	53
Standard Deviation	119	57	51
Mean Wind Speed	21.5	14.1	15.2
Sample Size	16	192	98

Table 4. 2.25m observations (StickNet) gust factor (3-sec/10-min) statistics (A), longitudinal turbulence intensity (TI) statistics (B), and longitudinal integral length scale statistics (C) for smooth, open, and roughly open exposures stratified by precipitation structure (convective/ stratiform) and eyewall or outer-vortex. The mean wind speed (m s^{-1}) for each group is also included.

A.

Statistic	Eyewall	Outer Vortex - Stratiform	Outer Vortex- Convective
Gust Factor- Smooth			
Mean	1.43	1.47	1.51
Maximum	1.69	1.91	1.89
Minimum	1.26	1.11	1.24
Standard Deviation	0.08	0.09	0.09
Mean Wind Speed	22.2	13.2	14.5
Sample Size	130	2452	1845
Gust Factor – Open			
Mean	1.57	1.64	1.66
Maximum	1.74	2.27	2.16
Minimum	1.33	1.39	1.31
Standard Deviation	0.09	0.11	0.11
Mean Wind Speed	17.5	10.4	10.1
Sample Size	21	761	599
Gust Factor – Roughly Open			
Mean	N/A	1.80	1.82
Maximum	N/A	2.23	2.33
Minimum	N/A	1.41	1.47
Standard Deviation	N/A	0.13	0.14
Mean Wind Speed	N/A	7.9	7.8
Sample Size	1	164	156

B.

Statistic	Eyewall	Outer Vortex - Stratiform	Outer Vortex- Convective
TI- Smooth			
Mean	0.16	0.18	0.18
Maximum	0.21	0.21	0.21
Minimum	0.12	0.08	0.10
Standard Deviation	0.02	0.02	0.02
Mean Wind Speed	22.2	13.2	14.5
Sample Size	130	2452	1845
TI – Open			
Mean	0.23	0.23	0.23
Maximum	0.26	0.26	0.26
Minimum	0.21	0.21	0.21
Standard Deviation	0.01	0.01	0.01
Mean Wind Speed	17.5	10.4	10.1
Sample Size	21	761	599
TI – Roughly Open			
Mean	N/A	0.28	0.28
Maximum	N/A	0.31	0.31
Minimum	N/A	0.26	0.26
Standard Deviation	N/A	0.01	0.02
Mean Wind Speed	N/A	7.9	7.8
Sample Size	1	164	156

C.

Statistic	Eyewall	Outer Vortex - Stratiform	Outer Vortex – Convective
Longitudinal Integral Scale- Smooth			
Mean	114	70	92
Maximum	591	561	833
Minimum	24	10	12
Standard Deviation	80	43	53
Mean Wind Speed	22.2	13.2	14.5
Sample Size	130	2452	1845
Longitudinal Integral Scale – Open			
Mean	69	66	70
Maximum	633	415	576
Minimum	18	18	17
Standard Deviation	131	50	51
Mean Wind Speed	17.5	10.4	10.1
Sample Size	21	761	599
Longitudinal Integral Scale – Roughly Open			
Mean	N/A	54	59
Maximum	N/A	352	284
Minimum	N/A	9	11
Standard Deviation	N/A	55	46
Mean Wind Speed	N/A	7.9	7.8
Sample Size	1	164	156

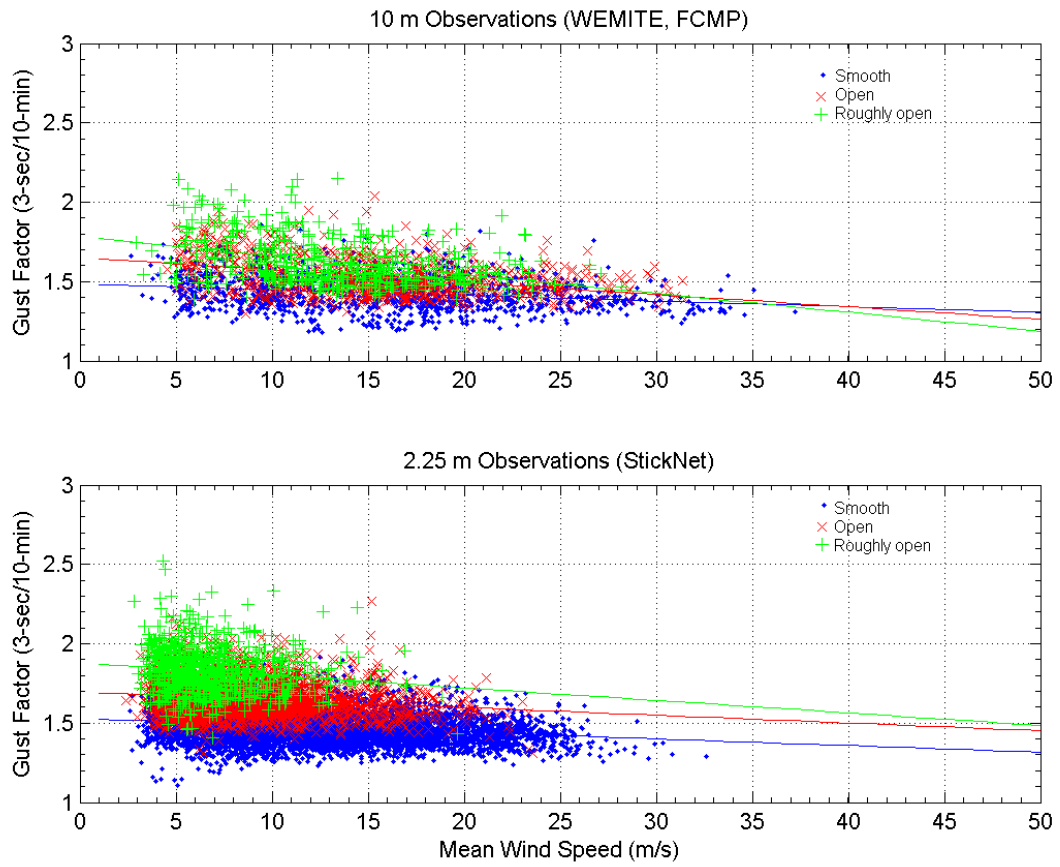
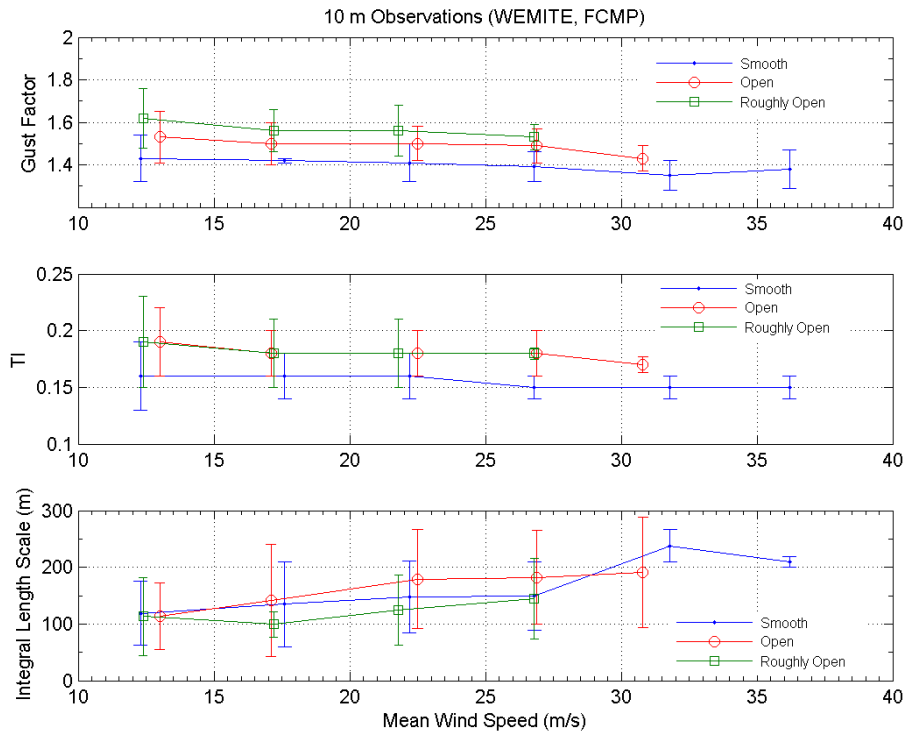


Figure 1. Observed 3-second/10-minute gust factors for 10 m (top) and 2.25 m (bottom) observations for smooth (blue), open (red), and roughly open (green) exposure categories. The linear trend line is provided for each observing height and exposure category.

A.



B.

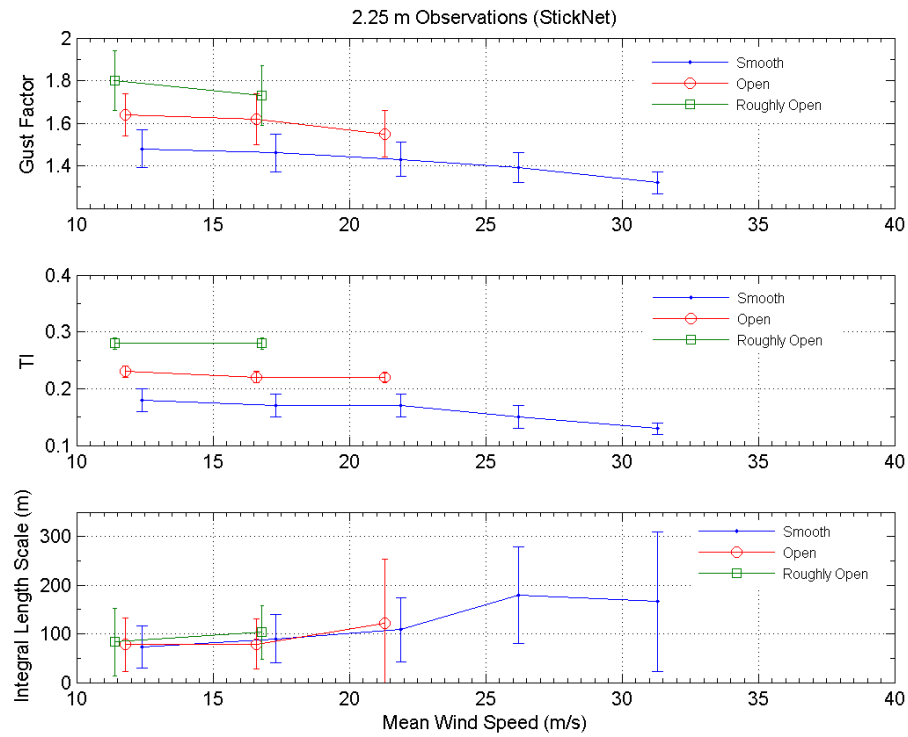


Figure 2. Mean values of gust factor (top), longitudinal turbulence intensity (middle), and longitudinal integral length scale (bottom) for 10 m (A) and 2.25 m (B) observations, shown as a function of mean wind speed for smooth (blue), open (red), and roughly open (green) exposure classifications. Errorbars represent ± 1 standard deviation from the mean.

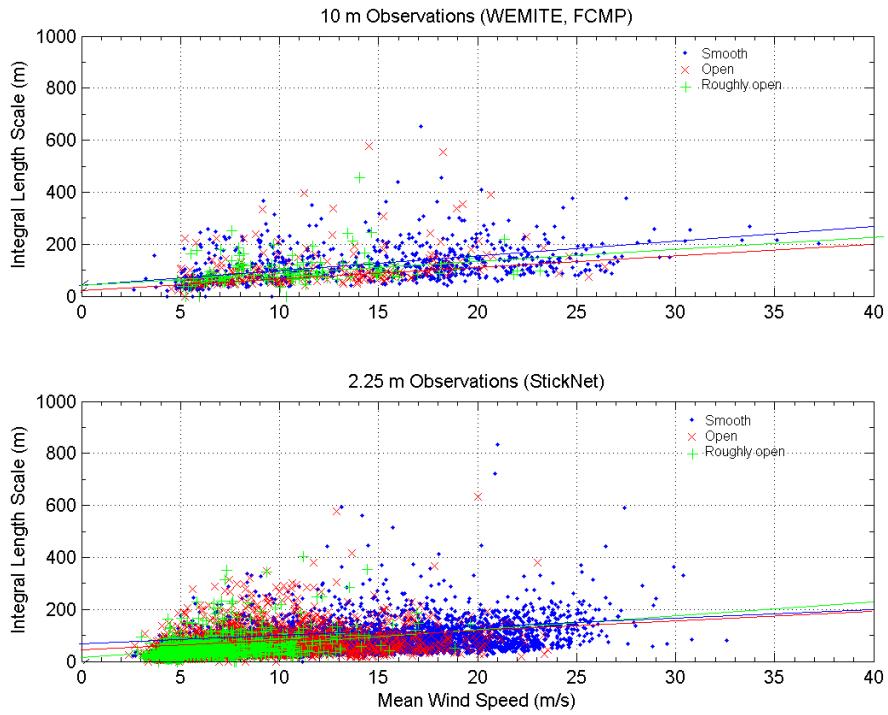


Figure 3. 10 m (top) and 2.25 m (bottom) longitudinal integral length scales shown as a function of 10-minute mean wind speed for smooth (blue), open (red), and roughly open (green) exposure classifications.

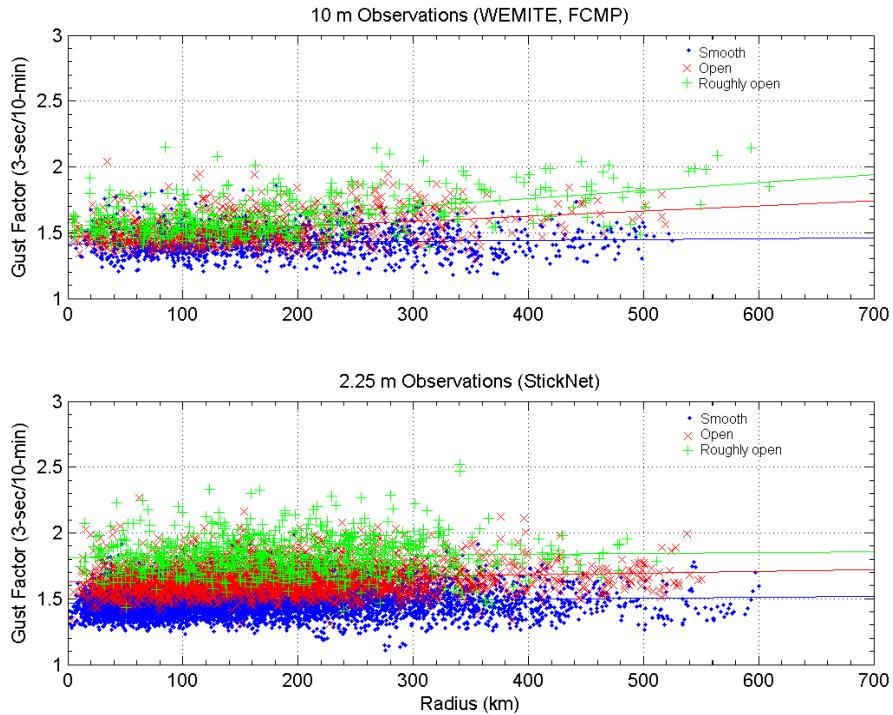


Figure 4. 10 m (top) and 2.25 m (bottom) gust factor (3-sec/10-min) observations for smooth (blue), open (red), and roughly open (green) exposure classifications shown as a function of radial distance. The linear trend line for each exposure classification is provided.

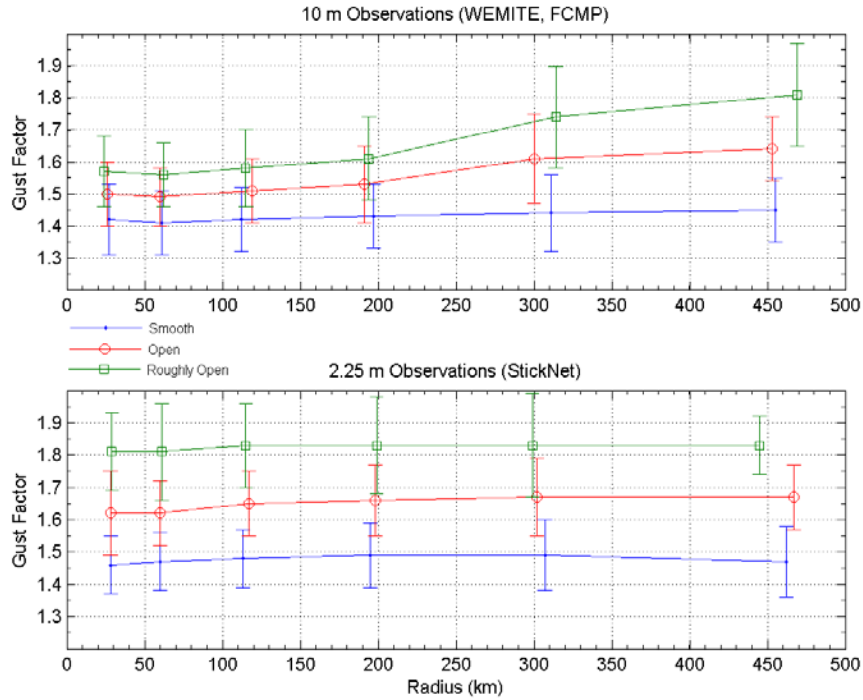


Figure 5. 10 m (top) and 2.25 m (bottom) mean gust factors for radial groups for smooth (blue), open (red), and roughly open (green) exposure classifications. Error bars represent ± 1 standard deviation from the mean value for each group.

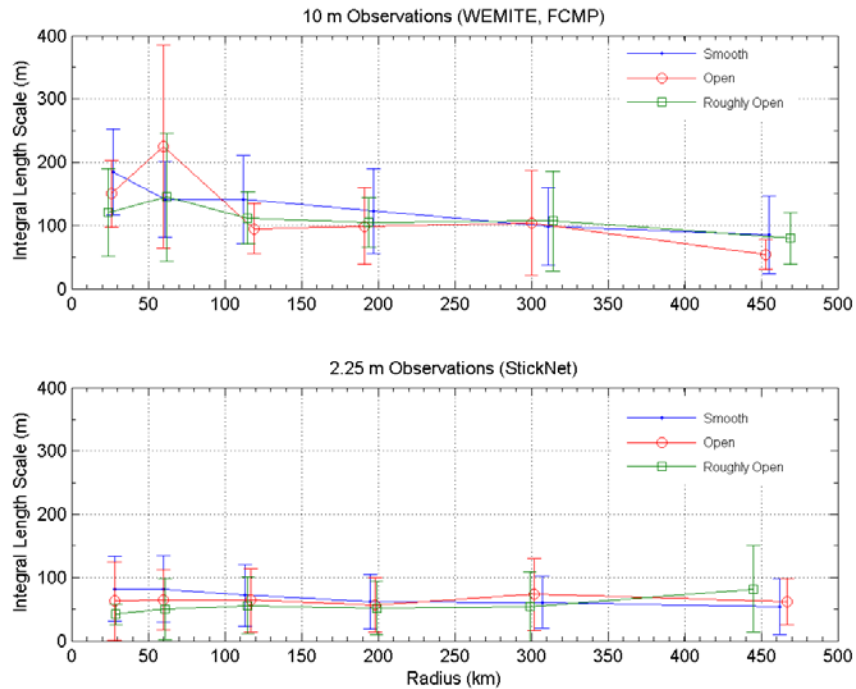


Figure 6. 10 m (top) and 2.25 m (bottom) mean longitudinal integral length scale values for smooth (blue), open (red), and roughly open (green) exposure group classifications, for radial groups. Error bars represent ± 1 standard deviation from the mean value for each group.

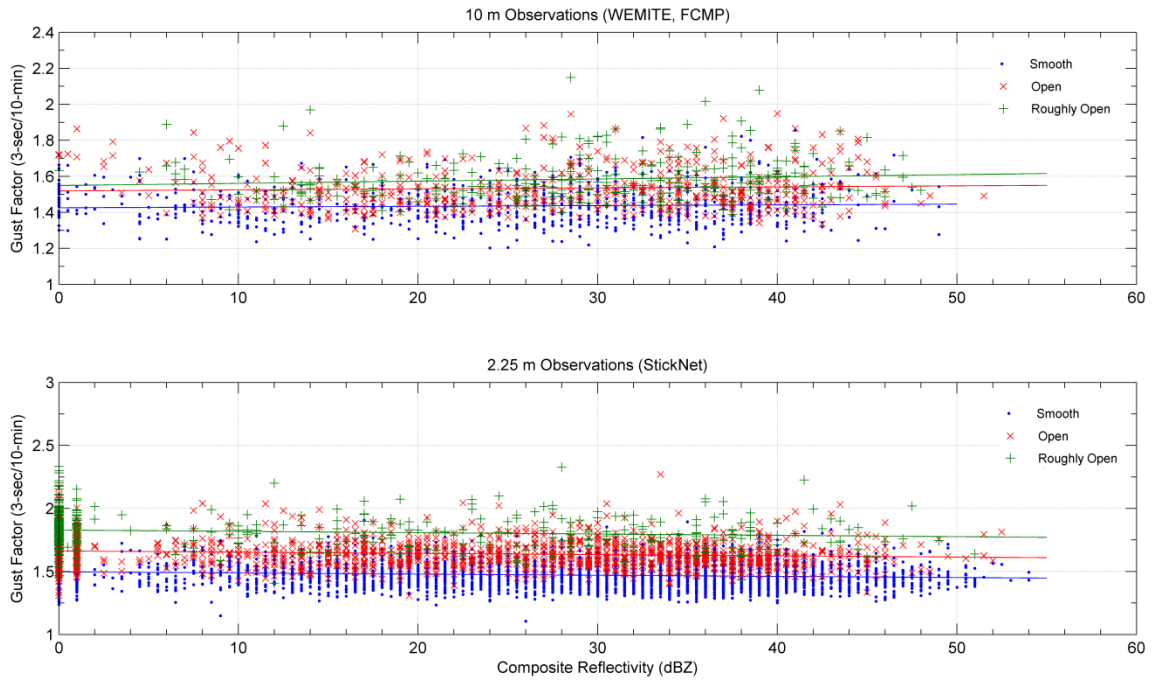


Figure 7. 10 m (top) and 2.25 m (bottom) gust factors for smooth (blue, open (red), and roughly open (green) exposure classifications shown as a function of composite reflectivity value. The linear trend line for each exposure classification is provided.